Journal of Materials Science and Engineering, Vol. 38, No. 1, PP. 49-55 (*2006*)

Thermal Dissipation Performance of a Heat sink/ Vapor Chamber Prepared by Metal Injection Molding Process

金屬射出成形散熱片與蒸氣盒之散熱性質研究

B.Y. Chen*[1], K.S. Hwang, C.C. Wang[2]
陳柏源*[1]、黃坤祥、王青志[2]

隨著電子產品微小化後，散熱問題已成爲電子產業之一大挑戰。因此，冷卻技術的研發已日形重要。本先導型實驗以射出成形製程製作散熱片(Heat Sink)以及含有鰭片之蒸氣盒(Vapor Chamber)，並研究其散熱性質。由實驗得知，在不施加保壓之射出條件下，可以得到完整之散熱鰭片，且鰭片之高寬比可達到 17.6。而鰭片與底部燒結後之密度都在 96% 以上，此表示已無連通孔產生之顧慮，對於將熱迅速傳至鰭片之能力也較不受影響。在散熱性能方面，散熱鰭片之熱阻值大約爲 1.156°C/W，而在 Tj 溫度爲 70°C 時，所能負荷的功率爲 40W，而含有鰭片之蒸氣盒之熱阻值約爲 1.046°C/W。相信再增加鰭片數目、增大風扇效率、加大鰭片之高寬比後，此第一代之蒸氣盒之熱阻值將可再大幅降低。

關鍵詞：金屬粉末射出成形(MIM)、銅粉、散熱鰭片、蒸氣盒、熱管理

The heat dissipation has become one of the major challenges in current electronic packaging due to the ever-increasing high current density and high power in new electronic devices. In this research, a copper heat sink and copper vapor chamber that contain cooling fins were prepared using the metal injection molding (MIM) technology, and their heat dissipation performances were evaluated.

The results show that with optimized processing parameters, particularly the holding pressure, fins with an aspect ratio up to 17.6 could be produced. After sintering, the densities of the fin and the bottom plate were about 96%. With only 32 fins and a small fan installed, the thermal resistance of the heat sink was 1.156°C/W, and the power dissipation was 40W when the junction temperature was at 70°C. The efficiencies of the vapor chamber that contained copper powder wick at the bottom and wire meshes on the top of the chamber, the thermal resistance was decreased to 1.046°C/W.

Keywords: Metal Injection Molding(MIM), Copper Powders, Heat sink, Vapor Chamber, Heat Dissipation.

＃本文轉載自 2005 年中國材料科學學會材料年會論文集。
[1]*Department of Materials Science and Engineering, National Taiwan University*
（[1] 台灣大學材料科學與工程學系）
[2]*Sintontech Corporation*
（[2] 興東昌精密工業股份有限公司）

1. Introduction

The directions in recent development of electronic packaging have been in making smaller, thinner, and lighter devices and with a high thermal dissipation capability[1]. With these goals, the thermal management of the electronic products have become a major challenge for the industry[2]. One of the possible solutions is the employment of vapor chambers, of which the large-area base is in contact with the heat source to provide a fast spreading of the heat generated by the heat source. Inside the chamber, the wick structure provides the heat dissipation like the heat pipe through the two-phase transformation of water. The water vapor is then condensed at the top plate, which is connected to the cooling fins with large surface areas[3,4].

In the conventional vapor chamber, the copper fins are soldered or brazed to the top plate of the box. These solder or brazed joints form a thermal barrier between the two adjacent copper components and deteriorate the overall heat dissipation performance. In this study, the metal injection molding (MIM) process was employed to prepare the vapor chamber with cooling fins without any secondary joining process in order to eliminate the thermal barrier[5,6]. However, the MIM process involves powder kneading, molding, debinding, and sintering, which could introduce contaminations and deteriorate the inherent high thermal conductivity of copper[7]. The objective of this study was to thus to fabricate a MIM vapor chamber that incorporates cooling fins with large aspect ratios and to evaluate its thermal resistance.

Table. 1 The characteristics of the A635 copper powder

Designation	A635
Supplier	ACu Powder
Particle Size (μm) (Laser Scattering)	D_{90} = 38.2 D_{50} = 18.5 D_{10} = 9.4
Shape	Near Spherical
True Density (Pycnometer)	8.34 g/cm^3
Arnold Apparent Density	3.55 g/cm^3
Tap Density	4.17 g/cm^3
Oxygen contents (%)	0.170

2. Experimental Procedure

2.1 Materials and MIM Processes

The characteristics and the morphology of the copper powder used in this study are shown in Table 1 and Figure 1, respectively. To prepare the feedstock, a multi-component binder system with its composition shown in Table 2 was employed.

After kneading the copper powder and the binder, the feedstock was injection molded into a heat sink using an injection molding machine (Arburg 440C, Lossburg, Germany). As shown in

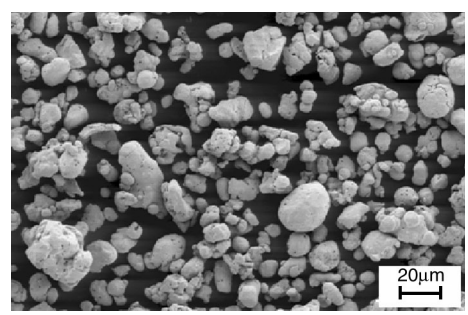

Fig. 1 The morphology of the A635 Cu powder under SEM

Table. 2 Compositions of the binder.

	Backbone	Filler	Surfactant 1	Surfactant 2
Composition (%)	40	54	3	3

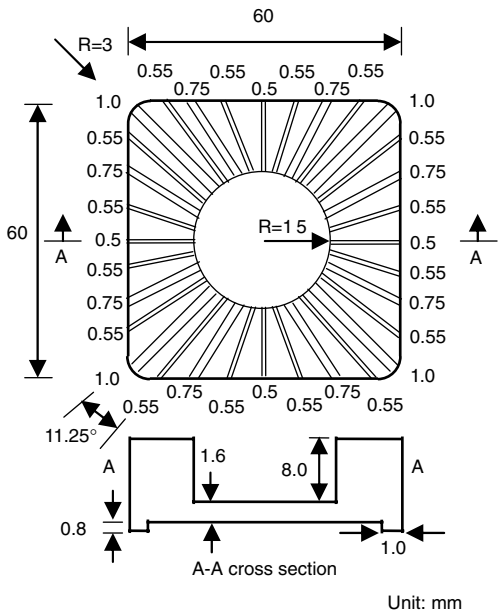

Fig. 2 The dimensions of the heat sink with 32 cooling fins

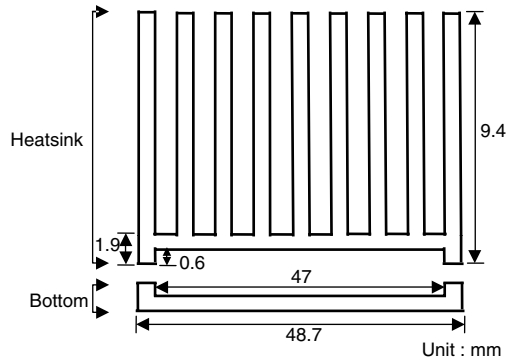

Fig. 3 The construction of the MIM vapor chamber

Table. 3 The characteristics of the 103A copper powder.

Designation	103A
Supplier	ACu Powder
Particle Size (μm) (Laser Scattering)	D_{90} = 131.2 D_{50} = 92.0 D_{10} = 64.2
Shape	Spherical
True Density (Pycnometer)	8.64 g/cm^3
Apparent Density	4.95 g/cm^3
Tap Density	5.43 g/cm^3
Flow Rate (sec./50g)	12.35
Oxygen contents (%)	0.402

Figure 2, the heat sink contained 32 fins, which were all 8.8 mm high but with four different thickness, 0.5, 0.55, 0.75 and 1.00mm. The corresponding aspect ratios were, 8.8, 11.7, 16.0, and 17.6, respectively. The molded green part was solvent debound in a heptane bath, thermally debound in hydrogen, and then sintered at 1050°C for two hours.

2.2 Vapor Chamber Construction

The upper element of the vapor chamber was made with the MIM heat sink. For the bottom element, the 32 cooling fins was cut off, as shown in Figure 3.

Two kinds of wick structure were used in this study. For the powder-mesh type, copper powders were loosely sintered at 850°C for one hour onto the bottom copper plate using the loose powder sintering process. The heating rate was 5°C/min. A copper mesh was then bent to the sawtooth shape and placed on top of the copper powder wick. The other wick structure was the mesh-mesh type, in which two sawtooth copper meshes were overlapped orthogonally and inserted into the chamber. The characteristics of the copper powder used for the wick were shown in Table 3. The morphologies of the copper powder and the copper mesh are shown in Figure 4.

After the wick structure had been constructed, the top and bottom plates were glued together using a regular mixture of epoxy and hardener. The assembled vapor chamber was then connected to pipes and valves, as shown in Figure 5, which were needed for vacuuming and water injection.

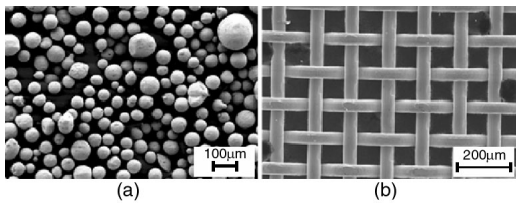

Fig. 4 The morphologies of the 103A Cu powder and copper mesh under SEM

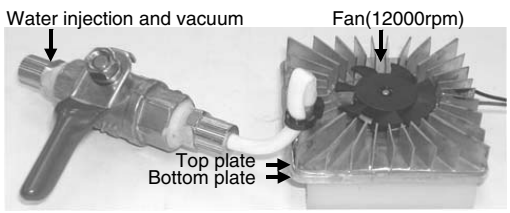

Fig. 5 The assembled vapor chamber for thermal resistance measurement

2.3 Thermal Resistance Measurement

To measure the thermal resistance, the temperature at the junction between the base of the vapor chamber and the heat source, which simulates the CPU, Tj, was measured using a thermocouple. The thermal resistance, θ, is calculated by the following equation:

$$\theta = (Tj-Ta)/Q$$

where Ta is the ambient temperature and Q is the heat supplied. The size of base of the vapor chamber was 48.7×48.7 (mm) and the size of the heater plate was 29.7×29.7 (mm). During the measurement, a thermal grease was applied between the base of vapor chamber and the heater. The thermal conductivity coefficient of the grease was 3.8 W/mK (T-Grease 2500, THERMAGON, Inc.).

3. Results

To mold successfully the heat sink with high aspect ratio fins, several parameters were adjusted, as shown in Table 4. With an optimized selection of processing parameters, the mold condition 3 was employed for the preparation of the MIM samples. The sintered densities of the fins were almost the same at about 96%, regardless of the thickness, as shown in Table 5. The densities of the base plates were also about 96%. This means that there should be no interconnected open pores in the specimen.

Table. 4 Molding conditions of the heat sink

Mold	1	2	3	4	5
Injection Pressure Limit (bar)	600	600	550	500	500
Holding Pressure (bar)	no	no	no	no	no
Injection Speed (ccm/s)	37.2	34.1	34.1	34.1	31.0
Dosage (ccm)	9.92	9.92	9.92	9.92	9.92
Mold Temp. (°C)	50	50	50	50	50
Nozzle Temp. (°C)	160	160	160	160	160
Cooling Time(s)	15	50	50	50	50
Defects ? (fin) (wall) (cold well)	 no no no	 no no yes	 no no no	 yes yes no	 yes yes no

To understand whether the part was debound and sintered properly, the contents of carbon, sulfur, oxygen, and nitrogen were measured after sintering. Table 6 shows that these elements were reduced significantly. The low carbon content implied that the debinding was complete. The low oxygen and nitrogen content also indicated that the sintering was carried out adequately. Since

Table. 5 Green and sintered densities of cooling fins with different thickness

Thickness of Fins (mm)	Green Density (g/cm^3)	Sintered Density (g/cm^3)
1	5.04	8.60 (95.98%)
0.75	5.04	8.63 (96.32%)
0.55(A)	5.11	8.61 (96.09%)
0.55(B)	5.11	8.63 (96.32%)
0.5	5.13	8.59 (95.87%)

Table. 6 The contents of C, S, O and N of the copper specimen removed at different processing stages

	Carbon (%)	Sulfur (%)	Oxygen (%)	Nitrogen (%)
A635 (as received)	0.019	0.003	0.170	0.007
Die Compact (sintered)	0.003	0.001	0.003	<0.001
Heat sink (sintered)	0.010	0.001	0.023	<0.001

impurities dissolved in copper could significantly deteriorate the thermal conductivity of copper, it was important to know whether the MIM process contaminated the copper. A comparison between press-and-sintered copper discs (12mm in diameter and 5mm thick) and MIM heat sink were conducted, and the impurity contents were measured by an Inductively Coupled Plasma with a Mass Spectrometer (ICP-Mass). The total amount of the residual elements measured was 1212 ppm, which was higher than the 483 ppm of the die compacted sample and the 299 ppm of the as received A635 powders. As shown in Table 7, the main impurity was Fe, Ti, and Sn, which could be caused by the wear from the kneading, molding, and sintering processes.

Figure 6 demonstrates the effects of wick

Table. 7 Impurities of sintered copper specimens prepared with die compaction and MIM process

Impurity (ppm)	A635 (as received)	Die Compact	Heat sink (MIM)
Al	3.4	3.5	6.3
Si	ND	11.7	18.0
Ti	ND	ND	251.5
Cr	ND	ND	32.6
Mn	3.2	5.2	22.1
Zn	14.2	11.9	5.3
Fe	16.0	55.0	225.0
Ni	43.0	45.4	48.6
Rh	28.5	29.5	26.8
Ag	41.6	46.7	65.9
Sn	149.0	274.0	510.0
Total	298.9	482.9	1212.0

structure and the amount of the water on the thermal performance when no fan was installed. In general, the powder-mesh wick was better than the mesh-mesh type. On the water content, it was clear that when the porous wick was 100% filled with water, the lowest thermal resistance would be attained. When a fan was installed, the thermal resistance of both wick structures decreased significantly, as shown in Figure 7.

With only 32 fins and 100% pores filled with water, the thermal resistance of the vapor chamber with the powder-mesh structure was 1.046 °C/W and the power dissipation was 42W when the junction temperature was 70°C. In contrast, the thermal resistance of the straight heat sink was 1. 156°C/W. This indicated that the phase transformation of water had occurred and enhanced the thermal dissipation of the chamber. When no water was in the wick, the thermal resistance was higher than that of the straight heat sink, or the top portion of the chamber. This was because the space inside the chamber impeded the

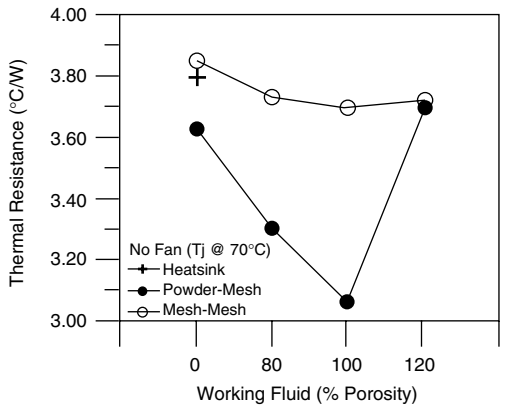

Fig. 6 Comparison on thermal resistance of vapor chambers with different wick structure and amount of water. (no fan installed).

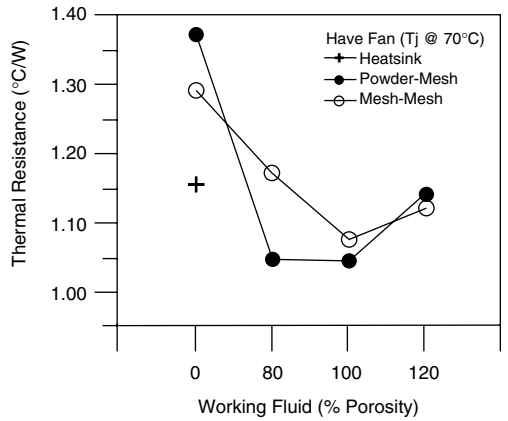

Fig. 7 Comparison on thermal resistance of vapor chambers with different wick structure and amount of water (with fan installed)

thermal conductivity. Both Figure 6 and Figure 7 also indicated that the water content is critical in obtaining the optimum thermal performance. When there was too much water, the radius of curvature of the water profile at the surface was quite flat. This reduced the capillary pressure to draw condensed water from the top plate to the evaporation end, or the bottom plate, of the chamber. When the working fluid was too low, dry-out phenomena occurred and impaired the thermal dissipation capability.

4. Discussion

This study demonstrated that the thermal barrier, the solder joint at the bottom of the cooling fins, in conventionally assembled vapor chamber could be eliminated through the use of the MIM process. This process, however, must be employed with care because metallic contaminations, particularly Fe, occur during the kneading and molding steps. To reduce the contamination and the thermal resistance, special attention must be paid in the selection of the material for the kneader and the barrel and screw in the molding machine.

The above results show that, when all pores in the powder-mesh wick were filled with water and a small fan installed, the thermal resistance was 1.046 °C/W, and the power dissipation was 42W when the junction temperature was 70°C. This result indicated that the vapor chamber provides extra thermal dissipation capability compared to the straight heat sink. The benefits may not seem significant because there are only 32 cooling fins in the device. However, this study demonstrates that it is possible to mold and sinter successfully cooling fins with a sintered thickness of 0.42mm and an aspect ratio of 17.6. It is believed that more cooling fins with even higher aspect ratios can be produced. With the increased number of fins and larger areas of the cooling surfaces, the thermal resistance can be further reduced.

5. Conclusion

The fabrication of a copper vapor chamber that includes 32 fins was attempted in this study using the metal injection molding process. With adjusted processing parameters, 0.42mm thick cooling fins with an aspect ratio of 17.6 can be produced successfully. This demonstrates that the solder or brazed joint between the cooling fin and

the base plate in the conventional vapor chamber can be eliminated. Using a powder-mesh structure as the wick and adjusted amount of water, a thermal resistance of 1.046 °C/W was attained, and the power dissipation was 42W when the junction temperature was 70°C. It is believed that with increased number and higher aspect ratio of the cooling fins, the thermal performance can be further improved.

Acknowledgement

The authors are thankful for the financial support of this work provided by the SintonTech Corporation. The technical support on the evaluation of the thermal performance provided by DELTA ELECTRONICS Inc. is also gratefully acknowledged.

References

1. M. J. Ellsworth, "Chip Power Density and Module Cooling Technology Projections for the Current Decade, " Thermal and Thermomechanical Phenomena in Electronic Systems, 2 (2004) 707-708.
2. V. Wuttijumnong, T. Nguyen, M. Mochizuki, K. Mashiko, Y. Saito and T. Nguyen, "Overview Latest Technologies Using Heat Pipe and Vapor Chamber for Cooling of High Heat Generation Notebook Computer," Semiconductor Thermal Measurement and Management Symposium, Twentieth Annual IEEE, (2004) 221-224.
3. M. Vogel and G. Xu, "Low Profile Heat Sink Cooling Technologies for Next Generation CPU Thermal Designs," Electronics Cooling, 11(1) (2005).
4. J. Wei, A. Chan and D. Copeland, "Measurement of Vapor Chamber Performance," Semiconductor Thermal Measurement and Management Symposium, Ninteenth Annual IEEE, (2003) 191-194.
5. B. H. Shropshire, K. Klatt, S. T. Lin and T. Y. Chan, "Copper P/M in Thermal Management," The International Journal of Powder Metallurgy, 39(4) (2003) 47-50.
6. J. L. Johnson, P. Suri, D. C. Schoiack, R. Baijal, R. M. German and L. K. Tan, "Metal Injection Molding of High Conductivity Copper Heat Sinks," Advances in Powder Metallurgy & Particulate Materials: Part 8 Powder Injection Molding, (2003) 234-244.
7. W. J. Ullrich, "Fabrication of Copper P/M Structural Parts," The International Journal of Powder Metallurgy, 39(4) (2003) 40-46.